Electronic Supplementary Information

Reusable Polymer-Based Fluorescent Sensor Nanoprobe for Selective Detection of Cd^{2+} Ion in Real Water Sources
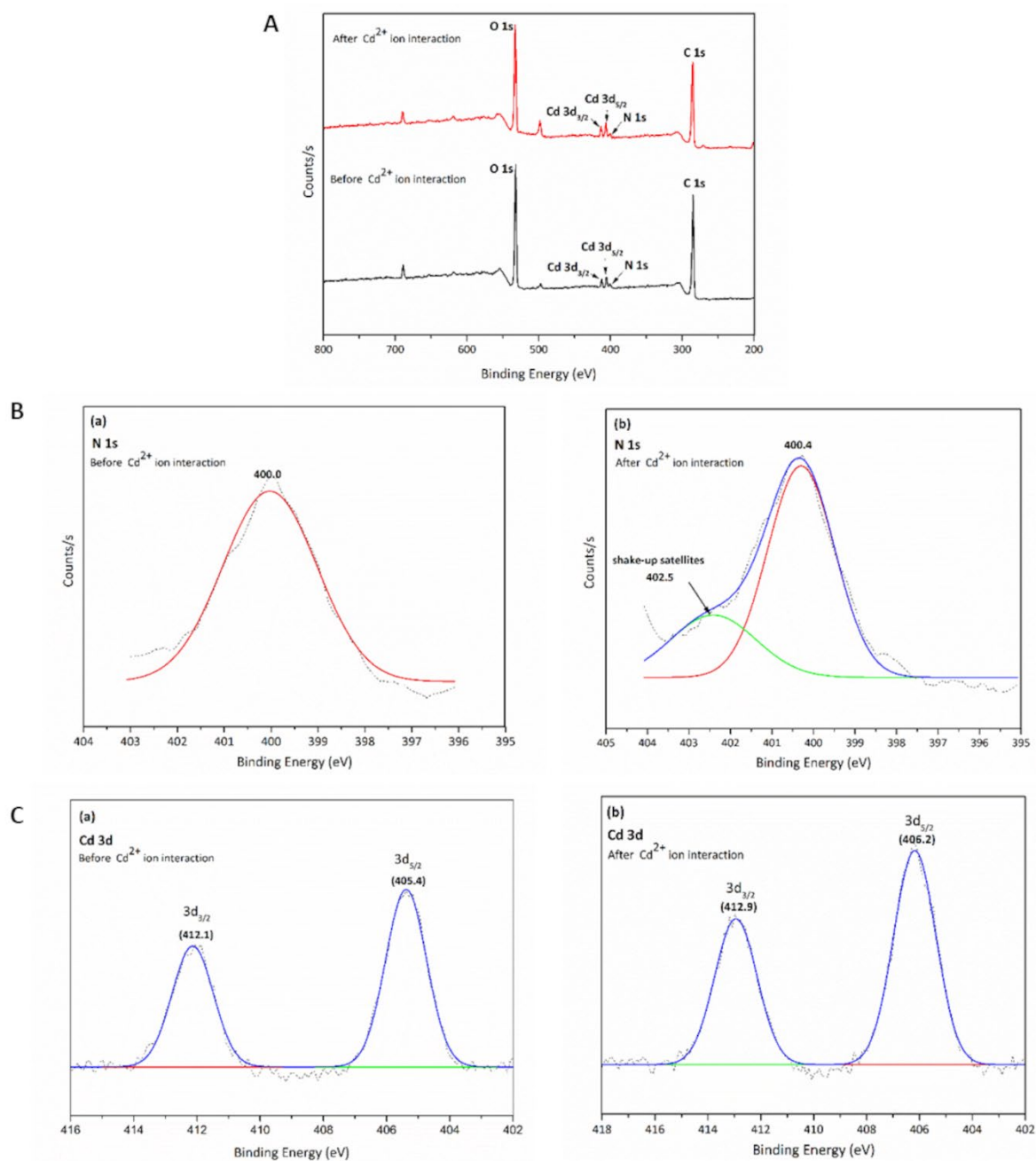
Merve Karabıyık*,[a] and Özgenç Ebil [b]

a,b Department of Chemical Engineering, Izmir Institute of Technology, 35430 Urla, Turkey,

* Correspondence: e-mail: merveozpirin@iyte.edu.tr

Table of Contents

1. X-Ray Photoelectron Spectroscopy (XPS) Analysis

Fig S1. XPS spectra A survey scans, B scans of N 1s (a and b) and C scans of Cd 3d (a and b) regions. (a) and (b) represent before and after Cd^{2+} ion interaction with QD-4AT nanoprobe, respectively.

Following the interaction of Cd^{2+} ion with QD-4AT nanoprobe, an electron transfer takes place between the nitroxide radical and Cd^{2+} ion. After the interaction with the $-NO^.$ free radical in 4AT, the electron cloud density in the nitroxide radical decreased due to the donation of the lone pair electrons in the radical to Cd^{2+} ion. As seen in the Fig. S1B(b), after the interaction with Cd^{2+}, the binding energies of N 1s shifted to higher binding energies because 4AT turned into a diamagnetic counterpart, which is oxoammonium cation, and the positive charge on

nitrogen causes the nitrogen electrons to bind more strongly to the atom. Therefore, the electrons are more difficult to remove and have a higher binding energy[1]. When the XPS results compared with each other before and after interaction with Cd^{2+}, a new peak having higher binding energy at 402.5 eV was obtained corresponds to the shake-up satellites.

Cd peaks before and after the interaction of QD-4AT nanoprobe with Cd^{2+} ions are shown in Fig. S1C(a) and (b). The binding energies of $Cd3d_{5/2}$ and $Cd3d_{3/2}$ sites were analyzed. The binding energies of $Cd3d_{5/2}$ and $Cd3d_{3/2}$ were in the range of 405.4- 406.2 eV and 412.1-412.9 eV, before and after the nanoprobe structure interaction with Cd^{2+}, respectively. The values before interaction are in good agreement with published data for CdTe[2,3]. However, the width values at the half-maximum after the interaction (2 eV) are higher than those for pure CdTe (1.5 eV), indicating that the interaction of the Cd^{2+} ion with the nanoprobe structure is successful. In addition, the shift of the peaks to the higher binding energy region after the interaction is also evidence of the interaction between Cd^{2+} ion and nanoprobe. These XPS results support the results of UV and FTIR analyses and show that a successful Cd^{2+} ion detection was achieved with the QD-4AT nanoprobe.

2. Fabrication of Cross-linked Copolymers via iCVD

Table S1. Details of GMA and V4D4 homo and copolymer depositions

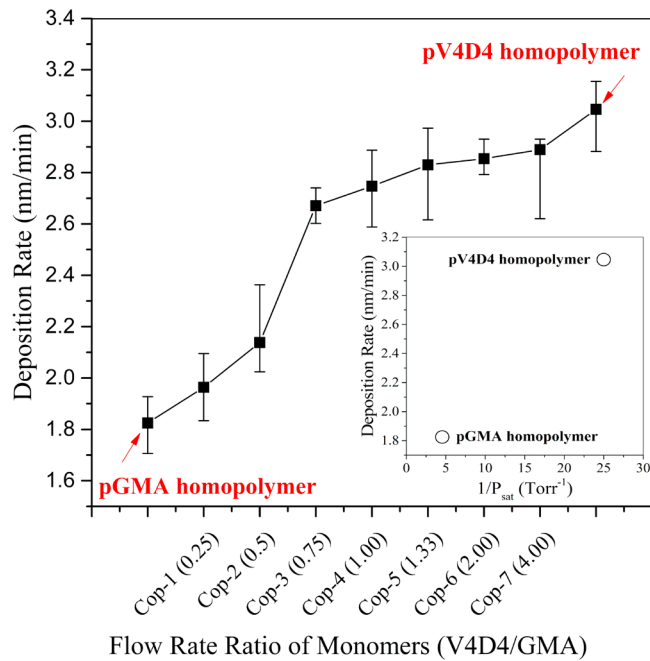| iCVD sample	Substrate Temp (°C)	Filament Temp (°C)	Pressure (mTorr)	Flow rate (sccm)			Flow Ratio (V4D4/GMA)	Deposition time (min)	Thickness (nm)
				V_4D_4	GMA	TBPO			
Homo pGMA				-	0.4		-		219.0±0.6
cop-1				0.1	0.4		0.25		235.7±0.4
cop-2				0.2	0.4		0.5		256.6±0.2
cop-3				0.3	0.4		0.75		320.5±0.4
cop-4	35	300	250	0.4	0.4	0.8	1.0	120	329.6±0.5
cop-5				0.4	0.3		1.33		339.5±0.3
cop-6				0.4	0.2		2.0		342.4±0.4
cop-7				0.4	0.1		4.0		346.8±0.4
Homo pV4D4				0.4	-		-		365.5±0.3

Fig. S2. Deposition rate of pGMA, pV4D4 and their copolymers.

3. Chemical Composition of Homo- and Cross-linked Copolymer Films

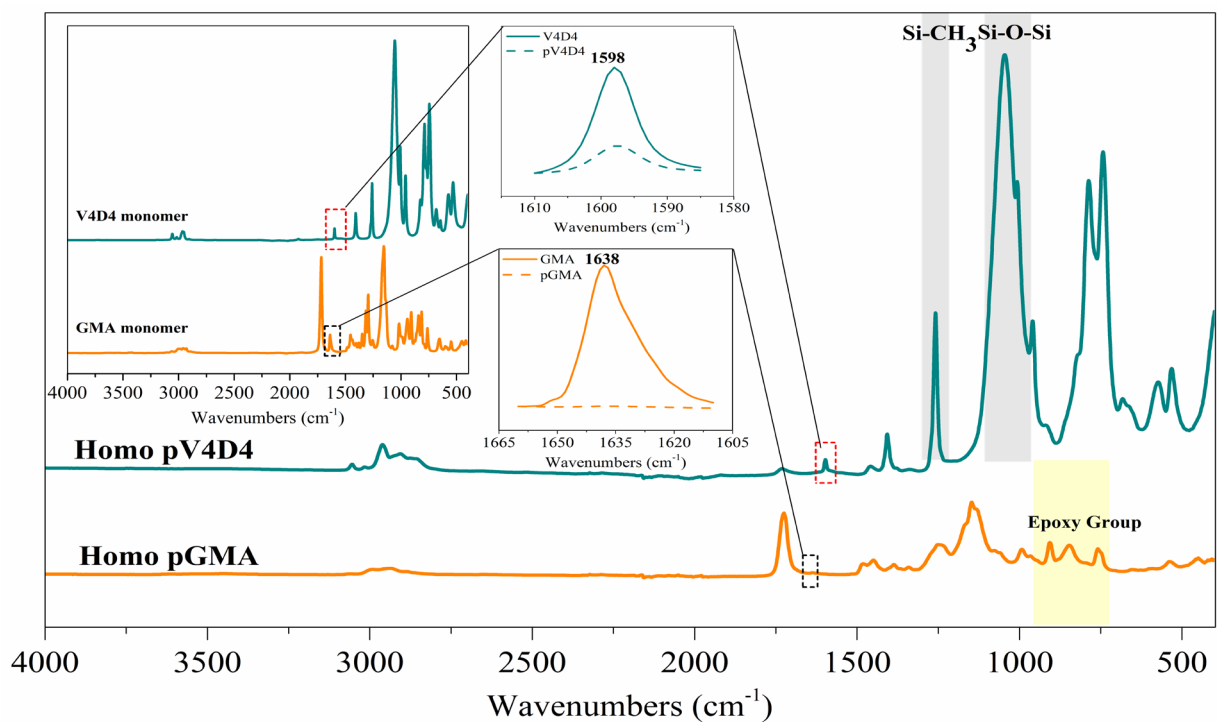## 3.1. Fourier Transform Infrared Spectroscopy (FTIR) Analysis

Fig. S3. FTIR spectra of GMA and V4D4 monomers and their homopolymer films.

The peak intensity of the V4D4 monomer at 1598 cm^{-1} attributed to the vinyl (CH$_2$=CH) group decreased to a certain extent in the pV4D4 spectrum. The decrease of the peak intensity demonstrates the consumption of vinyl functionality by polymerization of V4D4 monomer, but a significant amount of the vinyl group remained in the polymer. A V4D4 monomer contains 4 vinyl groups, and with free radical polymerization, complete consumption of the vinyl groups is unfeasible due to Specific peaks of V4D4 monomer, which are asymmetric (Si-O-Si) stretching (1075 cm^{-1}) and strong (SiCH$_3$) symmetric bending (1260 cm^{-1}), were obtained in pV4D4 spectrum similarly, and this is the indication of conserving the functionality of V4D4 monomer during deposition[4-6]. The prominent characteristic peaks between 3000 and 2800 cm^{-1} assigned to (C-H) symmetry and asymmetry stretching caused by (CH$_3$) and (CH$_2$) groups, and the peak at 1730 cm^{-1} related to carbonyl group (C=O) stretching vibration were explicitly observed in both GMA and pGMA spectra. The peak at 1640 cm^{-1} related to (C=C) bonds was not observed in iCVD deposited polymer's spectra, indicating polymerization[7-9]. The characteristic peaks at 906, 846, and 760 cm^{-1}, which belong to epoxy group stretching, were clearly seen in the pGMA spectrum in addition to the monomer spectra[10-12]. This is a clear indication of preservation of the functional properties of the monomer after deposition.

After homopolymer films, FTIR analysis was also carried out for cross-linked copolymer films to investigate the effect of cross-linker density on the films (Fig. S4).
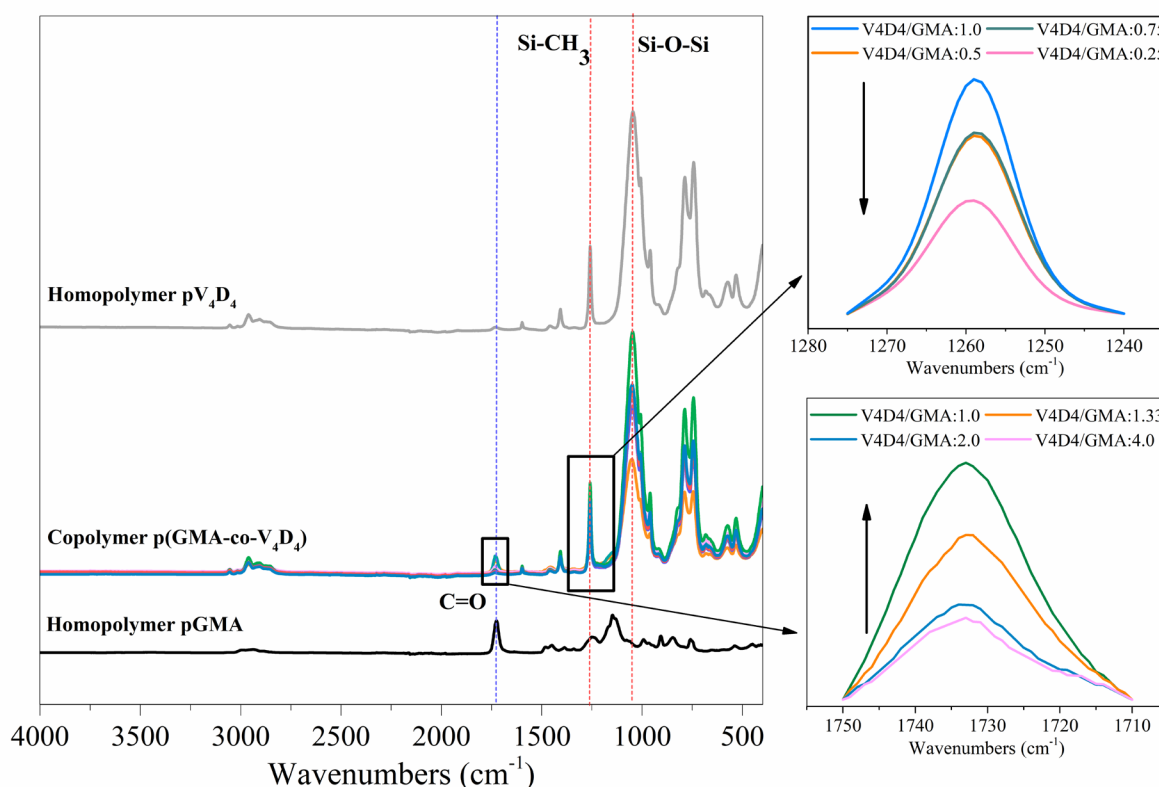
Fig. S4. FTIR spectra of pGMA and pV4D4 homopolymers and their copolymers.
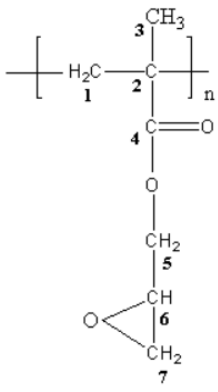
In copolymer FTIR spectra, all characteristic peaks of pV4D4 and pGMA homopolymers, including asymmetric (Si-O-Si) stretching (1075 cm^{-1}), strong (Si-CH$_3$) symmetric bending (1260 cm^{-1}) and (C=O) stretching

(1730 cm^{-1}) were observed. This is the evidence of the successful fabrication of cross-linked copolymer films in iCVD process. In Fig. S4, the FTIR spectrum of the copolymer films for two different peak regions has been magnified. The upper one was created by enlarging the area containing the (Si-CH$_3$) symmetric bending (1260 cm^{-1}), which is the specific peak of pV4D4. The spectra indicated the direct proportion effect of cross-linker density on copolymer deposition (gradually decreasing of F_{V4D4}/F_{GMA} ratio from 1.0 to 0.25 causes decreasing in the peak intensity of pV4D4 at 1260 cm^{-1}). This verified that the copolymerization was carried out correctly in the iCVD system. The area based on the (C=O) stretching peak at 1730 cm^{-1} belonging to pGMA was also enlarged. The peak intensities increased as the F_{V4D4}/F_{GMA} ratio decreased gradually from 4.0 to 1.0, that is, as the cross-linker density decreased. As a result, the flow rate ratio changes (F_{V4D4}/F_{GMA}) directly affected the content of copolymer films.

3.2. Nuclear Magnetic Resonance Spectrometry (NMR) Analysis

Proton nuclear magnetic resonance (^{1}H) and carbon nuclear magnetic resonance (^{13}C) spectra were recorded at ambient temperature using a 400 MHz Varian NMR spectrometer. Deuterated chloroform (CDCl$_3$) and deuterodimethylsulphoxide-d$_6$ (DMSO-d$_6$) were used as solvents for pV4D4 and pGMA, respectively.

Table S2. ^{1}H and ^{13}C NMR chemical shifts, δ (ppm), and signal assignments of pGMA in DMSO-d$_6$ at 25°C

pGMA	^{1}H NMR	Chemical shift δ (ppm)	^{13}C NMR	Chemical shift δ (ppm)
	H$_1$ (2H)	1.79	C$_1$	53.7
		1.86	C$_2$	44.2
	H$_3$ (3H)	0.70-1.20		44.6
				44.9
	H$_5$ (2H)	3.70	C$_3$	18.8
		4.27		16.8
				16.5
			C$_4$	177.4
				177.2
				176.3
	H$_6$	3.17	C$_5$	66.1
	H$_7$ (2H)	2.62	C$_6$	49.0
		2.77	C$_7$	40.3

The chemical shifts and signal assignments of the ^{1}H and ^{13}C NMR spectra are summarized in Table S2. All resonance signals have been assigned to the corresponding atoms according to the chemical structure given in the table. The assignments were made by comparing the spectra with those of analogous chemical groups reported in the literature for pGMA homopolymer[13,14]. The peaks observed prominently in the ^{1}H NMR spectrum indicate methyl (CH$_3$) and methylene (CH$_2$) groups in the polymer chain. The peak at 3.17 ppm is assigned to CH in the epoxy group of pGMA.

^{13}C NMR spectra indicate that the peak at 53.74 ppm is assigned to the methylene group (CH_2) labelled as C_1 in the polymer structure. Peaks were observed at around 44.16-44.94 ppm and 16.5-18.8 ppm, which were assigned to the second C in the figure above and methyl group (CH_3) in the polymer chain, respectively. The peaks around 176.33-177.37 ppm were assigned to the -C=O group carbon in the pGMA polymer film. The methylene group (CH_2) labelled as C_5 in the polymer structure was observed at 66.1 ppm. The dominant peaks of CH and CH_2 in the pGMA epoxy group were observed at about 48.99-49.34 ppm and 40.3 ppm, respectively. Similar results were obtained in the studies of Espinosa et al. (2001)[13] and Shah et al. (2015)[14].

Table S3. ^1H and ^{13}C NMR chemical shifts, δ (ppm), and signal assignments of pV4D4 in CDCl$_3$ at 25°C

pV4D4	^1H NMR	Chemical shift δ (ppm)	^{13}C NMR	Chemical shift δ (ppm)
	H_1	3.63	C_α	-0.85
	H_2	0.16-0.18		-0.89
	H_3	6.06	C_β	133.38-133.46
	H_4	5.94-5.99	C_λ	136.20

When the ^1H NMR results of pV4D4 homopolymer were analyzed in comparison with studies in the literature[15], the dominant peak was observed at around 0.16-0.18 ppm, which is attributed to methyl groups (CH_3) in the polymer chain. The prominent peak at around 5.94-5.99 ppm was assigned to CH_2, while the peak at 6.06 ppm was assigned to CH of the vinyl groups in the polymer chain. The small peak at 3.63 ppm during polymerization was assigned to OH groups at the ends of the polymer chains.

^{13}C NMR results of the pV4D4 polymer show that the peak located at approximately -0.85 and -0.89 ppm are attributed to the carbon of CH_3. The other two neighboring peaks that appear at around 133.46-133.38 and 136.20 ppm for the pV4D4 were assigned to CH_2 and CH of vinyl group, respectively.

When the ^1H and ^{13}C NMR results of the pGMA and pV4D4 homopolymer films were examined, it was found that the results supported the FTIR analysis and proved that the polymerization reactions took place successfully in the iCVD system.

4. Durability Test Results for Copolymer Films

Table S4. Chemical and mechanical durability test results.

iCVD sample	Resistance to Organic Solvent							Salt Resistance	Water Solubility	Adhesion
	Toluene	DCM	Ethanol	IPA	Acetone	DMF	THF			
pGMA								●	●	●
cop-1	●	●	●	●	●	●	●	●	●	●
cop-2			●	●	●	●		●	●	●
cop-3			●					●	●	●
cop-4	●		●	●		●		●	●	●
cop-5			●	●		●		●	●	●
cop-6			●	●		●		●	●	●
cop-7			●	●		●		●	●	●
pV4D4				●		●		●	●	●

● passed the test (result with less than 5% reduction in film thickness)

5. Energy-Dispersive X-ray Spectroscopy (EDX) Analysis

Table S5. EDX analysis before and after epoxy ring opening reaction of p(GMA-co-V4D4) copolymer film.

Element	p(GMA-co-V4D4)		Propylamine (1M)		Ethylenediamine (1M)		Ethylenediamine (10M)	
	Wt%	Atomic %	Wt%	Atomic %	Wt%	Atomic %	Wt%	Atomic %
C	52.40	59.46	52.10	59.02	51.72	58.53	37.17	42.79
O	47.60	40.54	45.88	39.02	44.52	37.82	39.20	33.88
N	-	-	2.02	1.96	3.76	3.65	23.63	23.33
Total	100.00	100.00	100.00	100.00	100.00	100.00	100.00	100.00

6. Comparison of Detection Limit of Sensor Nanoprobes for Cd^{2+} Ion

Table S6. Comparison of some recently reported fluorescent probes for Cd^{2+} detection

Sensing Probe	Linear Range (μM)	Detection limit (μM)	Reference
Thioglycerol (TG)-capped CdSe QDs	1-22	0.32	16
Ag_2S QDs	1-40	0.55	17
T(4-NO2-P)P[a]	1.0–10	0.28	18
Naphthalene-derived Schiff-base receptor (NIS)	0-30	0.39	19
Diarylethene derivative	0-35	2.3	20
Bis-TPE[b]	-	0.24	21
2-(Hydroxymethyl)quinolin-8-ol-based probe	-	1.18	22
Benzothiazole-based fluorescent probe	0-200	1.6	23
Polymer-QD-4AT	0.08-2.5	0.195	This work

a.T(4-NO2-P)P : Tetrakis(4-nitrophenyl)porphyrin
b.Bis-TPE: Thiourea-bridging bis-tetraphenylethylene

7. References

1. L. Ting, L. Sheng-Jian, J. Fang, R. Zi-Xuan, W. Li-Lian, Y. Xiang-Jun, T. Li-Hong and W. Shi-Xiong, *Nanoscale Research Letters,* 2019, 14:352.

2. X. Lu, X. Xingjian, Z. Wei, H. Qiaoyun and C. Wenli, *International Journal of Molecular Sciences*, 2015, **16**, 15670-15687.

3. O. Magdalena, W. Justyna and J. Krystyna, *Journal of Solid State Electrochemistry*, 2013, **17**, 2477-2486.

4. Y. Yoo, J. B. You, W. Choi and S. G. Im, Polymer Chemistry, 2013, **4**, 1664-1671.

5. J.-H. Seok, S. H. Kim, S. M. Cho, G.-R. Yi and J. Y. Lee, Macromolecular Research, 2018, **26**, 1257-1264.

6. D. Abessolo Ondo, F. Loyer, F. Werner, R. Leturcq, P. J. Dale and N. D. Boscher, ACS Applied Polymer Materials, 2019, **1**, 3304-3312.

7. F. Sarıipek and M. Karaman, Chemical Vapor Deposition, 2014, **20**, 373-379.

8. R. Bakker, V. Verlaan, C. H. M. van der Werf, J. K. Rath, K. K. Gleason and R. E. I. Schropp, Surface and Coatings Technology, 2007, **201**, 9422-9425.

9. M. Karaman and N. Çabuk, Thin Solid Films, 2012, **520**, 6484-6488.

10. Y. Mao and K. K. Gleason, Langmuir, 2004, **20**, 2484-2488.

11. Y. Mao and K. K. Gleason, Macromolecules, 2006, **39**, 3895-3900.

12. S. Mohammed Safiullah, K. Abdul Wasi and K. Anver Basha, Materials Letters, 2014, **133**, 60-63.

13. M.H. Espinosaa, P.J.O. del Torob and D.Z. Silva, *Polymer*, 2001, **42**, 3393–3397.

14. P. N. Shah, N. Kim, Z. Huang, M. Jayamanna, A. Kokil, A. Pine, J. Kaltsas, E. Jahngen, D. K. Ryan, S. Yoon, R. F. Kovar and Y. Lee, *RSC Advances*, 2015,**5**, 38673-38679.

15. D. E. Kherroub, M. Belbachir and S. Lamouri, *Research on Chemical Intermediates*, 2017, **43**, 5841-5856.

16. N. B. Brahim, N. B. H. Mohamed, M.Echabaane, M. Haouari, R. B. Chaâbane, M. Negrerie and H. B. Ouada, *Sensors and Actuators B: Chemical*, 2015, **220**, 1346–1353.

17. Q. Wu, M. Zhou, J. Shi, Q. Li, M. Yang and Z. Zhang, *Analytical Chemistry*, 2017, **89**, 6616–6623.

18. R. Khani, E. Ghiamati, R. Boroujerdi, A. Rezaeifard, M. H. Zaryabi, *Spectrochimica Acta Part A: Molecular and Biomolecular Spectroscopy*, 2016, **163**, 120–126.

19. J. H. Wang, Y. M. Liu, J. B. Chao, H. Wang, Y. Wanga and S.M. Shuang, *Sensors and Actuators B: Chemical*, 2020, **303**, 127216.

20. S. Peng, J. Lv, G. Liu, C. Fan and S. Pu, *Tetrahedron*, 2020, **76**, 131618.

21. S. Jiang, S. Chen, Z. Wang, H. Guo and F. Yang, *Sensors and Actuators B: Chemical*, 2020, **308**, 127734.

22. Y. Dai, K. Yao, J. Fu, K. Xue, L. Yang and K. Xu, *Sensors and Actuators B: Chemical*, 2017, **251**, 877–884.

23. J. Li, Y. Chen, T. Chen, J. Qiang, Z. Zhang, T. Wei, W. Zhang, F. Wang and X. Chen, *Sensors and Actuators B: Chemical*, 2018, **268**, 446–455.